Invest Ophthalmol Vis Sci. Author manuscript; available in PMC 2008 December 01.

Published in final edited form as:
Invest Ophthalmol Vis Sci. 2004 December ; 45(12): 4409–4414. doi:10.1167/iovs.04-0719.

Identification and spatiotemporal characterisation of spontaneous Ca^{2+} sparks and global Ca^{2+} oscillations in retinal arteriolar smooth muscle cells

Tim M. Curtis[1], **James Tumelty**[1,2], **Jennine Dawicki**[1], **C. Norman Scholfield**[2], and **J Graham McGeown**[2]

[1]Ophthalmic Research Centre, The Queen's University of Belfast, Institute of Clinical Sciences, The Royal Victoria Hospital, Grosvenor Road, Belfast BT12 6BA. N. Ireland. [2]Smooth Muscle Group, The Queen's University of Belfast, Medical Biology Centre, 97 Lisburn Road, Belfast, BT9 6BL. N. Ireland.

Abstract

Purpose—To identify spontaneous Ca^{2+} sparks and global Ca^{2+} oscillations in microvascular smooth muscle cells (MVSM) within intact retinal arterioles and to characterize their spatiotemporal properties and physiological functions.

Methods—Retinal arterioles were mechanically dispersed from freshly isolated rat retinae and loaded with the Ca^{2+}-sensitive dye Fluo-4. Changes in $[Ca^{2+}]_i$ were imaged in MVSM cells in situ using confocal scanning laser microscopy in XY or line scan mode.

Results—XY scans revealed both discretely localised, spontaneous Ca^{2+} events resembling Ca^{2+} sparks, and more global and prolonged Ca^{2+} transients which sometimes led to cell contraction. In line-scans, Ca^{2+} sparks were similar to those previously described in other types of smooth muscle with an amplitude ($\Delta F/F_0$) of 0.81±0.04 (mean±SE), Full Duration Half Maximum (FDHM) of 23.62±1.15 ms, Full Width Half Maximum (FWHM) of 1.25±0.05μm and frequency of 0.56±0.06 s^{-1}. Approximately 35% of sparks had a prolonged tail (>80ms), similar to Ca^{2+} 'embers' described in skeletal muscle. Sparks often summated to generate global and prolonged Ca^{2+} elevations on which Ca^{2+} sparks were superimposed. These sparks occurred more frequently (2.86±025 s^{-1}) and spread further across the cell (FWHM=1.67±0.08μm), but were smaller ($\Delta F/F_0$ = 0.69±0.04).

Conclusions—Retinal arterioles generate Ca^{2+} sparks whose characteristics vary during different phases of the spontaneous Ca^{2+}-signalling cycle. Sparks summate to produce sustained Ca^{2+}-transients associated with contraction and thus may play an important excitatory role in initiating vessel constriction. This deserves further study, not least because Ca^{2+} sparks appear to inhibit contraction in many other smooth muscle cells.

Introduction

As with all vascular systems, blood flow through the retinal circulation depends on the perfusion pressure gradient across the vascular bed and the resistance to flow within it. Importantly, vascular resistance is inversely related to the fourth power of the radius of a blood vessel. Thus, a small change in diameter has a substantial influence on the blood flow.

Corresponding author: Dr G McGeown, Smooth Muscle Group, The Queen's University of Belfast, Medical Biology Centre, 97 Lisburn Road, Belfast, BT9 6BL. UK, Email: g.mcgeown@qub.ac.uk, Tel: +44 (0)28 90972090.

Variation in vessel diameter occurs frequently and may be considered the main regulatory mechanism controlling flow in the retinal circulation1. The retinal arterioles provide the major site of resistance to blood flow in the retina and thus have the greatest capacity for regulation of retinal perfusion2. Alterations in retinal arteriolar tone occur through the contraction or relaxation of the microvascular smooth muscle cells (MVSM) in the wall of the vessels. The retinal vasculature is not innervated3, and retinal arteriolar tone is mainly regulated by local factors, such as variations in pO_2, pCO_2 and pH as well as mediators released from neighboring endothelial and retinal cells (e.g. nitric oxide and endothelin-1)1. These local influences combine to ensure that blood flow to the retinal tissue is closely matched to metabolic demand.

Although some of the local factors responsible for regulating retinal vessel diameter have been identified, as listed above, the complex cellular mechanisms that underlie changes in retinal MVSM tone are poorly understood. MVSM contractility is known to be heavily dependent on changes in $[Ca^{2+}]_i$4.5 We have previously shown that retinal MVSM cells possess a variety of Ca^{2+} handling mechanisms which modulate cytosolic $[Ca^{2+}]$, including voltage-dependent and store-operated Ca^{2+} influx channels6, pools of releasable Ca^{2+} (the sarcoplasmic reticulum (SR) Ca^{2+} stores)7 and multiple Ca^{2+} efflux pathways8.

Our previous studies were largely restricted to the measurement of average retinal MVSM $[Ca^{2+}]_i$. The application of confocal Ca^{2+}-imaging techniques have demonstrated, however, that intracellular $[Ca^{2+}]_i$ signals are not homogenously distributed and rises in $[Ca^{2+}]_i$ can differ in respect to their spatiotemporal properties and physiological functions. Both local and global Ca^{2+} signalling events have been observed in vascular smooth muscle cells and these may be generated spontaneously9 or in response to agonist exposure10,11. Localised Ca^{2+} transients are thought to result from the opening of clusters of ryanodine sensitive Ca^{2+} release channels on the SR and have been termed Ca^{2+} sparks. By activating Ca^{2+}-activated K^+ channels (K_{Ca}) to generate spontaneous outward currents (STOCs), Ca^{2+} sparks are thought to inhibit smooth muscle contraction in many tissues by increasing membrane polarisation and deactivating voltage-dependent Ca^{2+} channels, thus reducing Ca^{2+} influx12. In contrast to Ca^{2+} sparks, global Ca^{2+} oscillations have been implicated as mediators of constriction13. The frequency of these Ca^{2+} oscillations has been shown to increase with agonists that elevate inositol 1,4,5 trisphosphate (IP_3) levels, suggesting that Ca^{2+} release through IP_3 receptors on the SR contributes, at least in part, to their generation10,13.

The goal of the present study was to determine the spatiotemporal characteristics and functional relevance of spontaneous Ca^{2+}-transients in retinal MVSM by obtaining the first images from retinal arterioles of both localised and generalised Ca^{2+} signalling events. Furthermore, we show that Ca^{2+} sparks can summate to produce sustained global Ca^{2+} oscillations, some of which are followed by cell contraction. This is consistent with a model in which local Ca^{2+} release events play an excitatory, rather than an inhibitory role in the retinal vasculature, and thus runs counter to current paradigms concerning the functional significance of Ca^{2+} sparks in vascular smooth muscle12. We also demonstrate the existence of two distinct populations of Ca^{2+} sparks for the same release sites during different phases of spontaneous signalling, presumably reflecting changes in localised Ca^{2+}-release with different levels of cytoplasmic- and SR-$[Ca^{2+}]$.

Methods

Retinal microvessel preparation

Male Sprague-Dawley rats (200-300 g) were anaesthetized with CO_2 and killed by cervical dislocation. Animal use conformed to the guidelines of the ARVO statement for the Use of Animals in Ophthalmic and Vision Research and UK Home Office Regulations. Retinae

were rapidly removed and arterioles devoid of surrounding neuropile isolated as previously described7.6 In brief, retinal quadrants were lightly triturated using a fire polished Pasteur pipette (internal tip diameter 0.3 mm) in a low Ca^{2+} Hanks' solution. Homogenates were centrifuged at 3000 rpm for 1 min, the supernatant aspirated off and the tissue washed again with low Ca^{2+} medium. The remaining fragments were incubated at 21°C in 1 ml of low Ca^{2+} Hanks' solution containing 10 μM Fluo-4 AM (Molecular Probes, Eugene, OR) and the suspension agitated every 15 min for 2 h. This prolonged incubation was necessary to facilitate adequate loading of the retinal MVSM cells with Fluo-4.

Homogenates were diluted with 10 volumes of low Ca^{2+} medium and the mixture vigorously triturated. Of this mixture, 1 ml was pipetted into a rotatable circular glass-bottomed recording bath on the stage of an inverted microscope (Nikon Eclipse TE300). Microvessels were anchored down with tungsten wire slips (50 μm diameter, 2 mm length) and superfused with normal Hanks' solution at 37°C. The recording bath was rotated so that the long axis of the arterioles was parallel to the x-axis of the microscope. Drug solutions were delivered via a 5-way micro-manifold with an exchange time of ~ 1 s, as measured by switching to a dye solution.

Solutions

The bath solution had the following composition (in mM): 140, NaCl; 5, KCl; 5, D-glucose; 2, $CaCl_2$; 1.3, $MgCl_2$; 10, HEPES, pH 7.4 with NaOH. Low Ca^{2+} medium differed only in that it contained 0.1 mM $CaCl_2$.

Ca^{2+} imaging and data analysis

Changes in $[Ca^{2+}]_i$ were imaged in MVSM cell arrays with a confocal scanning laser microscope (Bio-Rad, MR-A1) used in X-Y mode at a rate of 1 image per 1.2s and in line scan mode at a rate of 500 scans/s14. Confocally imaged microvessels were excited at 488 nm and emitted light was filtered through a 530- to 560-nm band-pass filter. Data acquisition was controlled with Timecourse software (Lasersharp™; Biorad, US) and images were processed and analyzed with Image J (NIH, US). Confocal fluorescence data (F) were normalized using the average resting fluorescence (F_0) for periods that exhibited no spontaneous elevations in $[Ca^{2+}]_i$.

Ca^{2+} sparks were measured within regions of interest (ROIs; 4μmx4μm boxes in XY mode and 4μmx120ms boxes in line scan mode), while global Ca^{2+} oscillations were averaged across the entire cell. Ca^{2+} events were defined as an increase in F/F_0 of > 2 standard deviations above the mean resting fluorescence. The amplitudes of Ca^{2+} sparks and global Ca^{2+} oscillations were taken as the maximum increase in normalized fluorescence ($\Delta F/F_0$). Ca^{2+} event durations were measured along a line through the peak fluorescence as the time elapsed from reaching half the maximum amplitude during the rising phase, to falling back to that value during the decay, i.e., the full duration at half-maximal fluorescence (FDHM). Spatial spread was similarly defined as the distance in micrometers between the half-maximal fluorescence rise on either side of the peak fluorescence, i.e., the full width at half-maximum (FWHM). In some experiments using XY scan mode, cell area was calculated using the area calculator plug-in for Image J (Wayne Rasband, NIH).

Values are expressed as means ± SE. Comparisons were made with unpaired Student's *t*-tests, with $p<0.05$ considered significant.

Results

Identification of Ca^{2+} sparks and global Ca^{2+} oscillations in retinal MVSM cells

To explore whether distinct sub-cellular Ca^{2+} transients exist in rat retinal MVSM cells, changes in fluorescence intensity were monitored by laser scanning confocal microscopy in myocytes still embedded within their parent arterioles and loaded with the Ca^{2+} indicator dye Fluo-4. For the purposes of this study recordings were confined to retinal arteriole segments that were 35-40 μm in diameter and these represent the main trunk arterioles that emanate from the optic disk6. The wall of isolated retinal arterioles consisted of a monolayer of MVSM cells surrounding an intact endothelium (Fig 1). Under resting conditions, vascular myocytes within freshly dispersed retinal arterioles demonstrated considerable Ca^{2+} signaling activity. Two main types of spontaneous $[Ca^{2+}]_i$ transients were observed, with different kinetics and spread. Brief and spatially localized events resembling Ca^{2+} sparks were often seen in close proximity to the cell membrane, as well as more prolonged global Ca^{2+} oscillations which usually spread across the full width of the cell (Fig 2).

Global Ca^{2+} oscillations precede retinal MVSM contraction

In arterial smooth muscle, global Ca^{2+} oscillations have been recognized as the main driving force underlying vasoconstriction13. Likewise we observed that spontaneous global Ca^{2+} oscillations in retinal MVSM cells could trigger contractile responses. In the example shown (Fig 3) a global Ca^{2+} oscillation was associated with a 19% reduction in MVSM cell area. Although it is apparent, therefore, that a prolonged global increase in $[Ca^{2+}]_i$ can trigger retinal MVSM contraction, this was relatively uncommon. In 6 vessels (82 cells), only 18 out of 103 global Ca^{2+} oscillations were followed by a decrease in cell area. The amplitude of the $[Ca^{2+}]_i$ increases were no higher in cells which contracted than in those which did not ($p=0.55$), so this variability probably reflects differences in the sensitivity of the individual cells to $[Ca^{2+}]_i$. Mechanical contraction was never observed in response to individual Ca^{2+} sparks (6 vessels, 82 cells, 163 sparks).

Line scan imaging reveals that Ca^{2+} sparks give rise to global Ca^{2+}oscillations

Although spontaneous $[Ca^{2+}]_i$ transients could be visualized in retinal MVSM cells using XY scan imaging, this approach did not allow adequate temporal resolution of rapid, localized $[Ca^{2+}]_i$ changes within a cell. Consequently, it appears from Fig 2B that both Ca^{2+} sparks and global Ca^{2+} oscillations have a similar time course. To improve temporal resolution the line-scan mode of confocal imaging was used. Analysis was limited to vessel segments exhibiting no frame-to-frame movement of the cells. A typical example of an image obtained by scanning a line orientated at right angles to the long axis of a cell is shown in Fig 4A. A brief, localised Ca^{2+} spark can be clearly seen in the image. This spontaneously localized Ca^{2+} event had a peak amplitude ($\Delta F/F_0$) of 0.95, a FDHM of 14 ms and was restricted to a relatively small area (FWHM of 1.57 μm). Interestingly some Ca^{2+} sparks (≅ 35% of recorded sparks in 7 cells) were associated with a prolonged tail (>80 ms) similar to that seen in the example in Fig 4A. These events resemble the Ca^{2+}-'embers' or 'glows' recently described in skeletal muscle cells15. Ca^{2+} embers were 'site dependent' and in some sites practically all Ca^{2+} sparks displayed prolonged tails.

It has been previously demonstrated in ileal myocytes that spatiotemporal recruitment of 'elementary' Ca^{2+} sparks may give rise to cell wide elevations in $[Ca^{2+}]_i$.16 Using line scan imaging it was possible to visualise the initiation site of some global Ca^{2+} oscillations in retinal MVSM cells. In the example shown in Fig 4B it is evident that a global Ca^{2+} oscillation was initiated from a site where spontaneous Ca^{2+} sparks were also observed. The temporal profile of the global Ca^{2+} oscillation consists of a series of step-like increases in fluorescence resulting from the summation of consecutive Ca^{2+} sparks. It is also striking that

even after the global Ca^{2+} oscillation reached its maximum, Ca^{2+} sparks persist throughout both the plateau and declining phases.

Analysis of spatiotemporal properties uncovers two populations of Ca^{2+} sparks

The spatiotemporal properties of Ca^{2+} sparks and global Ca^{2+} oscillations in retinal MVSM cells were characterized from line-scan images of 60 cells in 6 vessels, and the data are summarized in Table 1. Ca^{2+} sparks were separated into two groups, namely, 'basal' sparks that arose from resting fluorescence values (F/F_0 of 0.95-1.05) and those that were superimposed upon global Ca^{2+} oscillations (Ca^{2+} sparks on oscillations). At 0.81, the mean spark amplitude under basal conditions was nearly 6x the SD of the background signal noise (noise SD=0.138). Global Ca^{2+} oscillations were similar in amplitude to basal Ca^{2+} sparks, but were nearly 100-times longer in duration (as measured from the FDHM) and occurred less frequently (Table 1). Differences in the spatiotemporal properties of basal Ca^{2+} sparks and Ca^{2+} sparks overlaying Ca^{2+} oscillations were also observed. The latter were smaller in amplitude, increased in width and increased in frequency (Table 1).

Discussion

In this study we describe the first visualization of spontaneous subcellular Ca^{2+} transients in retinal arteriolar smooth muscle cells. Two distinct Ca^{2+} signaling events were seen, discretely localized, spontaneous near-membrane Ca^{2+} sparks and more global and prolonged Ca^{2+} oscillations. Most studies on elementary Ca^{2+} signaling events in arterial smooth muscle have used single, isolated myocytes, even though the ultimate goal is to understand how function is regulated in intact vessels10,17. A major advantage of the technique described here is the use of intact arteriole segments in which the physiological relationships between the retinal MVSM cells, basal lamina and endothelium are preserved. Our technique also allows simultaneous imaging of subcellular Ca^{2+} signals in a number of MVSM cells, thus allowing cell to cell variation to be assessed while increasing the amount of data that can be collected in a single experiment.

Ca^{2+} sparks are thought to result from transient local release of Ca^{2+} from intracellular stores and have been described in cardiac18, skeletal19 and several smooth muscle cell preparations12, including arteriolar smooth muscle cells20. In smooth muscle cells Ca^{2+} spark amplitudes are known to be quite variable, with the average peak increase in $[Ca^{2+}]_i$ ranging from 50-200 nM12. In retinal MVSM cells, the average spark amplitude ($\Delta F/F_0$ of 0.81; Table 1) equates to an elevation in $[Ca^{2+}]_i$ of ~80 nM as determined using the pseudoratiometric calculation of Cheng et al (1993)18, assuming an *in situ* dissociation constant for Fluo-4 of 1000 nM21 and a resting Ca^{2+} level in retinal arterioles of 66 nM7. The average frequency (0.56 s^{-1}), duration (23.6 ms; FDHM) and spatial spread (1.25μm FWHM) of Ca^{2+} sparks in retinal MVSM are all quite similar to those in other smooth muscle cells, with reported values for these parameters ranging from 0.5 to 1 s^{-1} 12, 30 to 65 ms22 and 1.2 to 2.3 μm23,24, respectively. There are, however, some reports of more prolonged Ca^{2+} sparks (100-600 ms) in tracheal25 and urinary bladder smooth muscle cells26, while the events observed in human cerebral arterial smooth muscle cells appeared to spread further, with an average FWHM of 8.2 μm 27.

Our records provide clear evidence that Ca^{2+} sparks in retinal MVSM cells may fuse to produce cell wide global Ca^{2+} oscillations that can lead to cell contraction. These findings are of particular interest since they imply that Ca^{2+} sparks in retinal arterioles are principally excitatory in nature, whereas it has been proposed that Ca^{2+} sparks exert a predominantly inhibitory effect in vascular smooth muscle, providing a negative feedback mechanism which favors decreased Ca^{2+} influx and vasodilatation12. Interestingly, only a small proportion of global Ca^{2+} oscillations actually led to retinal MVSM cell contraction. Ca^{2+}

ions regulate nearly every cell function and sub-cellular Ca^{2+} transients are known to cause a pulsatile activation of Ca^{2+} dependent enzymes28 as well as driving changes in gene expression29. Consequently, those Ca^{2+} oscillations that failed to initiate excitation-contraction coupling are still likely to be physiologically relevant.

Detailed analysis revealed two distinct populations of Ca^{2+} sparks, with those superimposed on global Ca^{2+} oscillations displaying an increased frequency and spread, but reduced amplitude, when compared with sparks originating at the same release sites but from basal $[Ca^{2+}]_i$ levels. Ca^{2+} sparks are thought to be generated by the opening of ryanodine receptor linked channels (RyRs) on the SR12, and elevations in cytosolic Ca^{2+} are known to increase RyR open probability30. This may well explain increased spark frequency during global Ca^{2+} oscillations. Likewise, increased spatial spread may also be accounted for by an overall increase in the open probability of RyRs, since this would favour recruitment of release sites. Since global Ca^{2+} oscillations in smooth muscle cells are known to involve Ca^{2+} store release13, the smaller amplitudes of the Ca^{2+} sparks seen during such oscillations in retinal MVSM cells may reflect a reduction in SR Ca^{2+} content. Clearly, further studies are now required to unravel the precise mechanisms through which localized Ca^{2+} release is modified during Ca^{2+} oscillations, as well as to determine the functional implications of such modifications.

Under basal conditions, many sparks in retinal MVSM cells had protracted tails similar to the Ca^{2+} embers of skeletal muscle cells15. We have previously described prolonged, spontaneous Ca^{2+} release events in isolated smooth muscle cells during store-overload14, but no such events have been reported in untreated smooth muscle, or indeed any intact tissue. In skeletal muscle cells, embers are thought to reflect direct RyR opening by voltage sensors15 but, since the RyRs are not believed to be under direct voltage control in smooth muscle, it is unclear what mechanism generates Ca^{2+} embers in retinal MVSM cells. It seems likely, however, that events in which Ca^{2+} release is prolonged well beyond the average channel-open time associated with RyRs in lipid bilayer experiments31 may have important consequences, perhaps increasing the likelihood of spark summation and the initiation of global Ca^{2+} oscillations. These findings also underline the fact that the study of intact tissues may reveal subtleties of signaling behaviour not apparent in isolated cells or molecules.

A possible limitation of our current model is the use of non-pressurized retinal arterioles. Passive stretching of the retinal vessel wall during increases in intraluminal pressure may lead to an elongation of the MVSM cells and thereby provoke changes in the spatiotemporal properties of the spontaneous Ca^{2+} signals. Increases in retinal MVSM cell length could modulate spontaneous Ca^{2+} sparks and global oscillations through the activation of stretch-activated currents32 or via stretch-induced gating of RyRs33. In rat cerebral arteries, pressurization increases the frequency of Ca^{2+} sparks and global Ca^{2+} oscillations, but other spatiotemporal features such as amplitudes and rise times are similar to those seen in non-pressurized vessels34.

In summary, the application of high resolution imaging to intact retinal arterioles has allowed us to visualize sub-cellular Ca^{2+}-signaling events in retinal MVSM cells. These cells are the primary effectors of retinal arteriolar tone and the data from the present study takes us a step closer to elucidating the basic mechanisms involved in the regulation of local blood flow in the retina. Understanding how such control is achieved will be fundamental to the development of novel therapeutic strategies aimed at restoring adequate blood flow in disease states such as diabetic retinopathy35 and glaucoma36.

Supplementary Material

Refer to Web version on PubMed Central for supplementary material.

Acknowledgments

We thank Fight for Sight (UK), The Wellcome Trust, The Juvenile Diabetes Research Foundation (US) and the British Heart Foundation for financial support.

References

1. Delaey C, Van D,V. Regulatory mechanisms in the retinal and choroidal circulation. Ophthalmic Res. 2000; 32:249–256. [PubMed: 11015035]
2. Hill DW. The regional distribution of retinal circulation. Ann R Coll Surg Engl. 1977; 59:470–475. [PubMed: 931327]
3. Ye XD, Laties AM, Stone RA. Peptidergic innervation of the retinal vasculature and optic nerve head. Invest Ophthalmol Vis Sci. 1990; 31:1731–1737. [PubMed: 1698744]
4. Guibert C, Beech DJ. Positive and negative coupling of the endothelin ETA receptor to Ca2+-permeable channels in rabbit cerebral cortex arterioles. J Physiol. 1999; 514(Pt 3):843–856. [PubMed: 9882755]
5. Hill MA, Zou H, Potocnik SJ, et al. Invited review: arteriolar smooth muscle mechanotransduction: Ca(2+) signaling pathways underlying myogenic reactivity. J Appl Physiol. 2001; 91:973–983. [PubMed: 11457816]
6. Curtis TM, Major EH, Trimble ER, et al. Diabetes-induced activation of protein kinase C inhibits store-operated Ca2+ uptake in rat retinal microvascular smooth muscle. Diabetologia. 2003; 46:1252–1259. [PubMed: 12898009]
7. Scholfield CN, Curtis TM. Heterogeneity in cytosolic calcium regulation among different microvascular smooth muscle cells of the rat retina. Microvasc Res. 2000; 59:233–242. [PubMed: 10684729]
8. Gormley BA, Scholfield CN. Mechanism of calcium extrusion in microvascular smooth muscle in the rat retina. J Physiology. 2004:555P.
9. Bolton TB, Gordienko DV, Pucovsky V, et al. Calcium release events in excitation-contraction coupling in smooth muscle. Novartis Found Symp. 2002; 246:154–168. [PubMed: 12164307]
10. Mauban JR, Lamont C, Balke CW, et al. Adrenergic stimulation of rat resistance arteries affects Ca(2+) sparks, Ca(2+) waves, and Ca(2+) oscillations. Am J Physiol Heart Circ Physiol. 2001; 280:H2399–H2405. [PubMed: 11299247]
11. Jaggar JH, Nelson MT. Differential regulation of Ca(2+) sparks and Ca(2+) waves by UTP in rat cerebral artery smooth muscle cells. Am J Physiol Cell Physiol. 2000; 279:C1528–C1539. [PubMed: 11029300]
12. Jaggar JH, Porter VA, Lederer WJ, et al. Calcium sparks in smooth muscle. Am J Physiol Cell Physiol. 2000; 278:C235–C256. [PubMed: 10666018]
13. Iino M, Kasai H, Yamazawa T. Visualization of neural control of intracellular Ca2+ concentration in single vascular smooth muscle cells in situ. EMBO J. 1994; 13:5026–5031. [PubMed: 7957068]
14. White C, McGeown JG. Inositol 1,4,5-trisphosphate receptors modulate Ca2+ sparks and Ca2+ store content in vas deferens myocytes. Am J Physiol Cell Physiol. 2003; 285:C195–C204. [PubMed: 12620813]
15. Gonzalez A, Kirsch WG, Shirokova N, et al. The spark and its ember: separately gated local components of Ca(2+) release in skeletal muscle. J Gen Physiol. 2000; 115:139–158. [PubMed: 10653893]
16. Gordienko DV, Bolton TB, Cannell MB. Variability in spontaneous subcellular calcium release in guinea-pig ileum smooth muscle cells. J Physiol. 1998; 507(Pt 3):707–720. [PubMed: 9508832]
17. Jaggar JH, Stevenson AS, Nelson MT. Voltage dependence of Ca2+ sparks in intact cerebral arteries. Am J Physiol. 1998; 274:C1755–C1761. [PubMed: 9611142]

18. Cheng H, Lederer WJ, Cannell MB. Calcium sparks: elementary events underlying excitation-contraction coupling in heart muscle. Science. 1993; 262:740–744. [PubMed: 8235594]
19. Tsugorka A, Rios E, Blatter LA. Imaging elementary events of calcium release in skeletal muscle cells. Science. 1995; 269:1723–1726. [PubMed: 7569901]
20. Burdyga T, Shmygol A, Eisner DA, et al. A new technique for simultaneous and in situ measurements of Ca2+ signals in arteriolar smooth muscle and endothelial cells. Cell Calcium. 2003; 34:27–33. [PubMed: 12767890]
21. Thomas D, Tovey SC, Collins TJ, et al. A comparison of fluorescent Ca2+ indicator properties and their use in measuring elementary and global Ca2+ signals. Cell Calcium. 2000; 28:213–223. [PubMed: 11032777]
22. Remillard CV, Zhang WM, Shimoda LA, et al. Physiological properties and functions of Ca(2+) sparks in rat intrapulmonary arterial smooth muscle cells. Am J Physiol Lung Cell Mol Physiol. 2002; 283:L433–L444. [PubMed: 12114206]
23. Furstenau M, Lohn M, Ried C, et al. Calcium sparks in human coronary artery smooth muscle cells resolved by confocal imaging. J Hypertens. 2000; 18:1215–1222. [PubMed: 10994752]
24. Pabelick CM, Sieck GC, Prakash YS. Invited review: significance of spatial and temporal heterogeneity of calcium transients in smooth muscle. J Appl Physiol. 2001; 91:488–496. [PubMed: 11408467]
25. Sieck GC, Kannan MS, Prakash YS. Heterogeneity in dynamic regulation of intracellular calcium in airway smooth muscle cells. Can J Physiol Pharmacol. 1997; 75:878–888. [PubMed: 9315357]
26. Herrera GM, Heppner TJ, Nelson MT. Voltage dependence of the coupling of Ca(2+) sparks to BK(Ca) channels in urinary bladder smooth muscle. Am J Physiol Cell Physiol. 2001; 280:C481–C490. [PubMed: 11171567]
27. Wellman GC, Nathan DJ, Saundry CM, et al. Ca2+ sparks and their function in human cerebral arteries. Stroke. 2002; 33:802–808. [PubMed: 11872907]
28. De Koninck P, Schulman H. Sensitivity of CaM kinase II to the frequency of Ca2+ oscillations. Science. 1998; 279:227–230. [PubMed: 9422695]
29. Cartin L, Lounsbury KM, Nelson MT. Coupling of Ca(2+) to CREB activation and gene expression in intact cerebral arteries from mouse : roles of ryanodine receptors and voltage-dependent Ca(2+) channels. Circ Res. 2000; 86:760–767. [PubMed: 10764409]
30. Saftenku E, Williams AJ, Sitsapesan R. Markovian models of low and high activity levels of cardiac ryanodine receptors. Biophys J. 2001; 80:2727–2741. [PubMed: 11371448]
31. Fill M, Copello JA. Ryanodine receptor calcium release channels. Physiol Rev. 2002; 82:893–922. [PubMed: 12270947]
32. Kirber MT, Walsh JV Jr. Singer JJ. Stretch-activated ion channels in smooth muscle: a mechanism for the initiation of stretch-induced contraction. Pflugers Arch. 1988; 412:339–345. [PubMed: 2459658]
33. Ji G, Barsotti RJ, Feldman ME, et al. Stretch-induced calcium release in smooth muscle. J Gen Physiol. 2002; 119:533–544. [PubMed: 12034761]
34. Jaggar JH. Intravascular pressure regulates local and global Ca(2+) signaling in cerebral artery smooth muscle cells. Am J Physiol Cell Physiol. 2001; 281:C439–C448. [PubMed: 11443043]
35. Schmetterer L, Wolzt M. Ocular blood flow and associated functional deviations in diabetic retinopathy. Diabetologia. 1999; 42:387–405. [PubMed: 10230642]
36. Flammer J, Orgul S, Costa VP, et al. The impact of ocular blood flow in glaucoma. Prog Retin Eye Res. 2002; 21:359–393. [PubMed: 12150988]

Europe PMC Funders Author Manuscripts

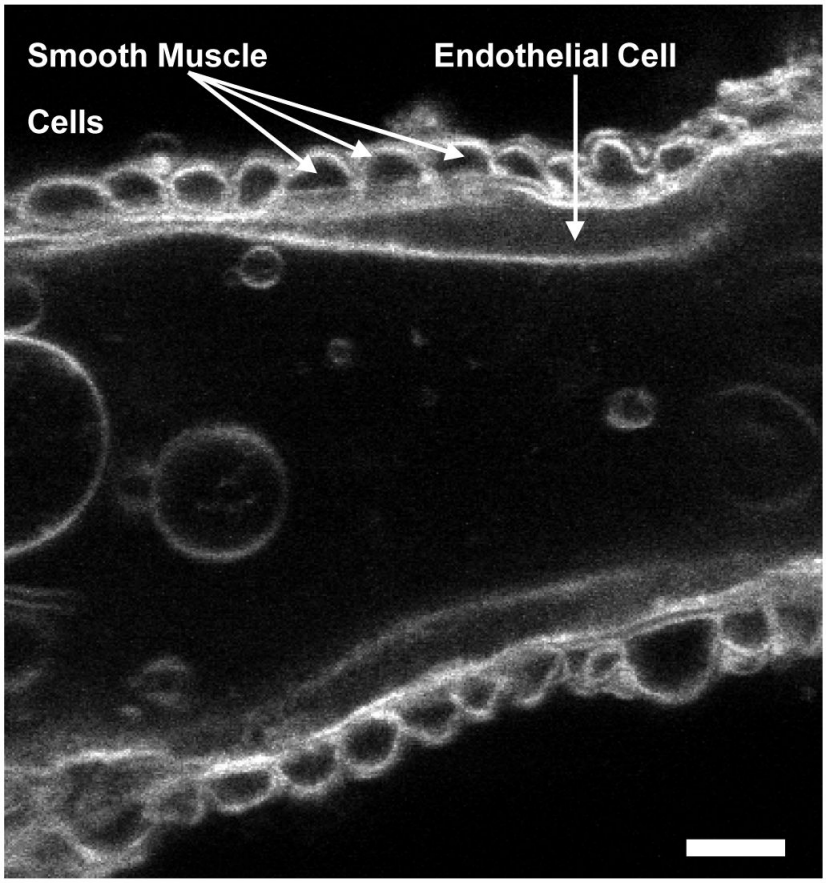

Fig 1.
Luminal confocal section of an isolated retinal arteriole loaded for 10 min with the membrane-tracking dye di-4-ANEPPS (10μM; Molecular Probes). Scale bar = 10 μm.

Europe PMC Funders Author Manuscripts

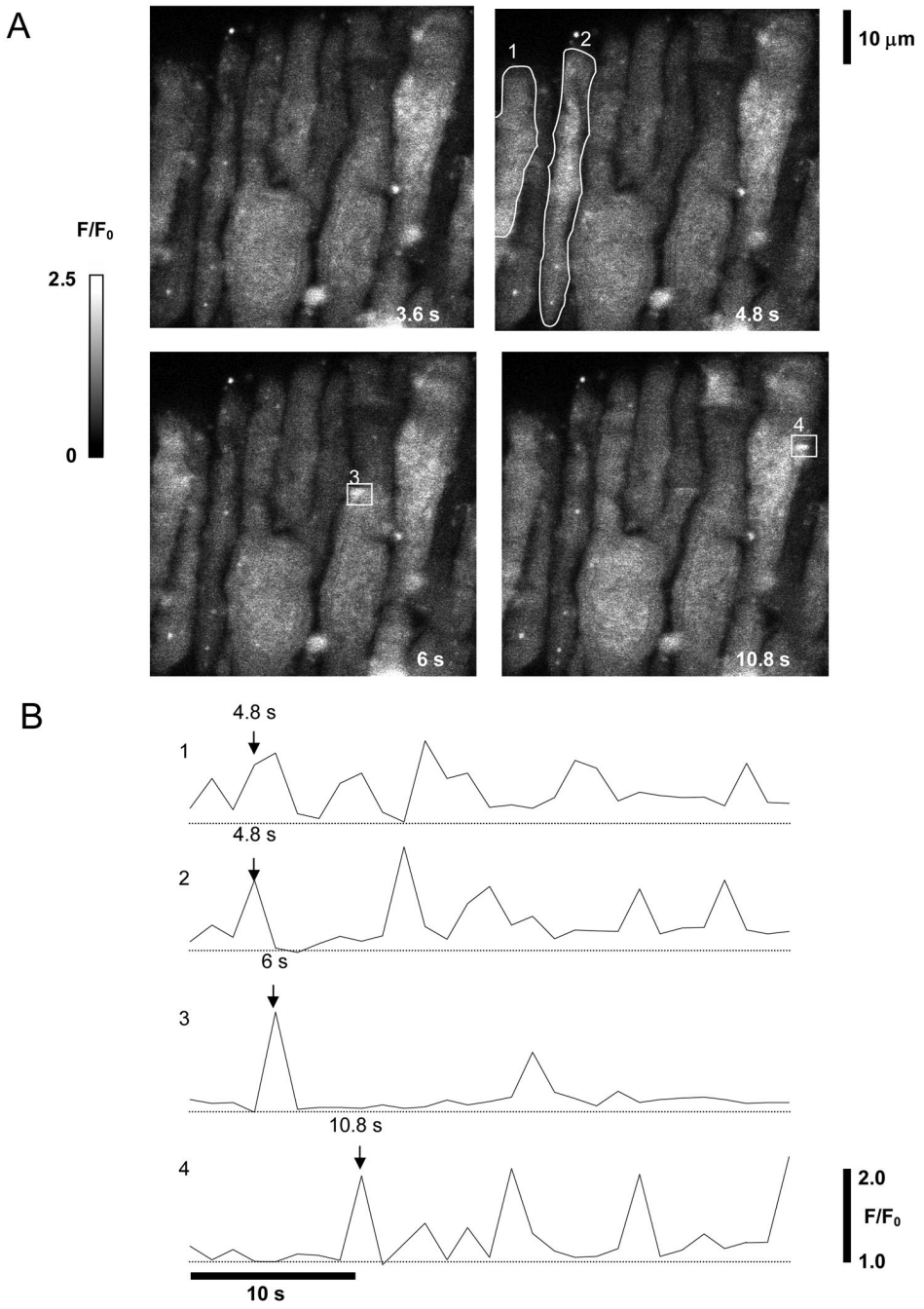

Fig 2.

Ca^{2+} sparks and waves imaged in fluo-4 loaded retinal MVSM cells. A. Four time frames from a series of XY images of a retinal arteriole. The smooth muscle cells are oriented at right angles to the long axis of the vessel. Fluorescence relative to basal values (F/F_0) is represented using a greyscale, as indicated on the calibration bar on the left. Four regions of interest (ROI) are marked and the average fluorescence within each of these regions through the course of the 40s experiment is plotted against time in B. The timepoint at which each frame was captured is indicated by labelled arrows. Both small localised events (ROIs 3 & 4), and generalised Ca^{2+} oscillations (ROIs 1 & 2), were seen. (A movie showing the spontaneous Ca^{2+} rises in this vessel is included as supplementary material online : Movie 1.

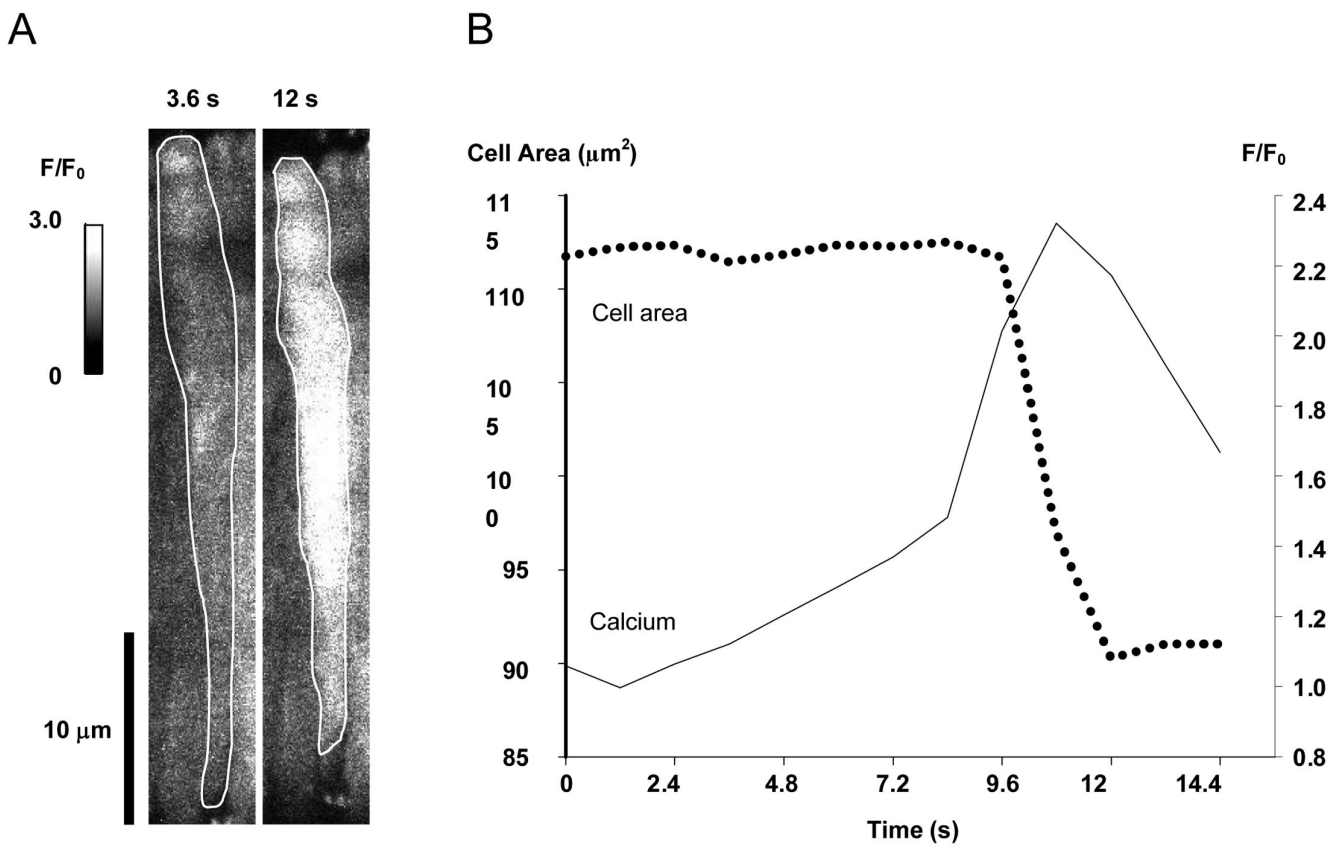

Fig 3.

Global Ca^{2+} oscillations can induce retinal MVSM cell contraction. A. The outline of a retinal arteriolar smooth muscle cell imaged prior to and during a global Ca^{2+} oscillation. B. Changes in calcium (as F/F_0) and cell area are plotted against time for the same cell.

Europe PMC Funders Author Manuscripts

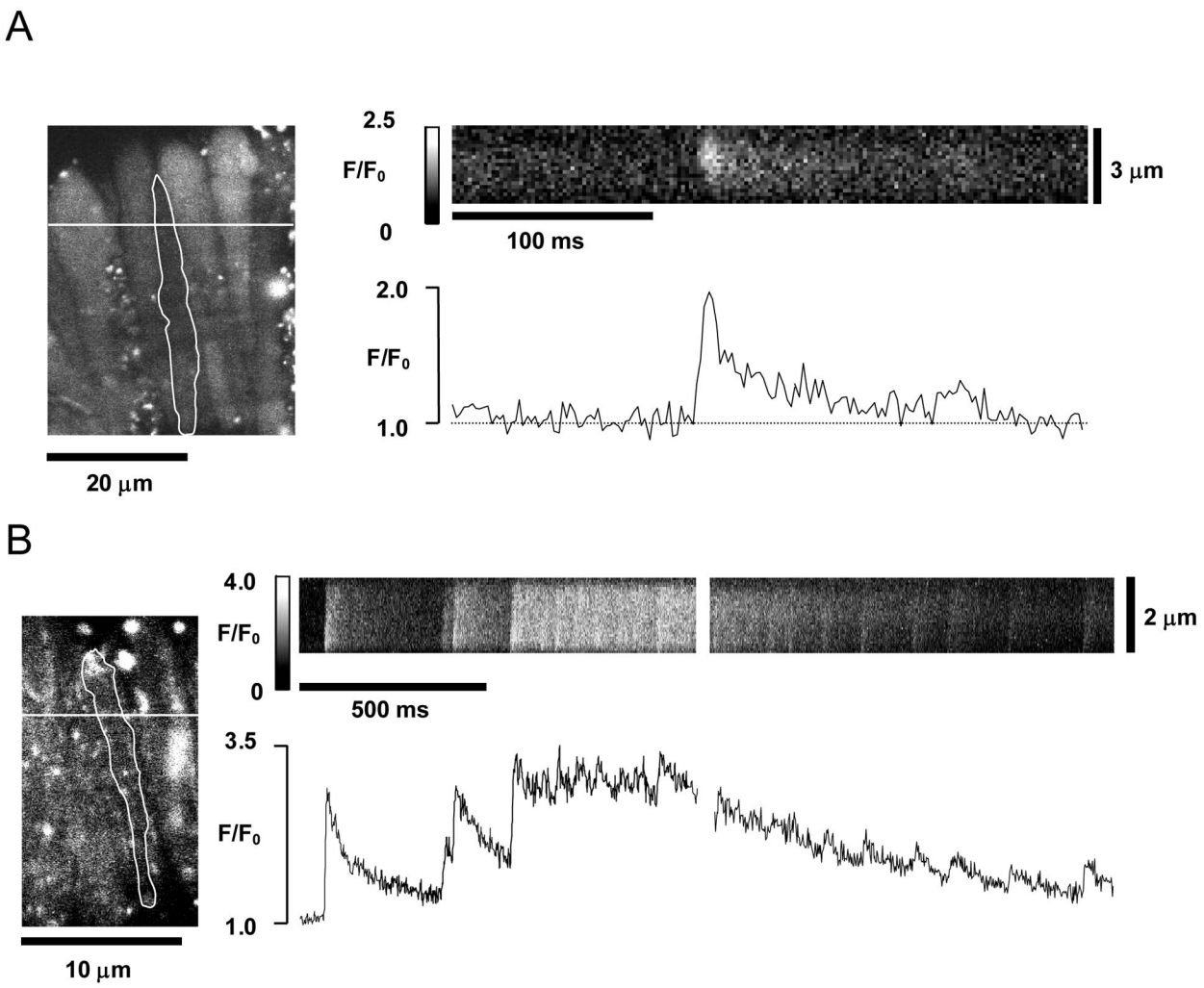

Fig 4.

Linescan images of Ca^{2+} sparks and global Ca^{2+} oscillations. A. The left-hand panel shows the shaded outline of a single retinal myocyte in a XY fluo-4 image of a retinal vessel. The position of the transverse scanline is marked, and the resulting line-scan image showing spontaneous changes in fluorescence for the selected cell is seen in the horizontal frame. Average fluorescence for this frame is plotted against time on the graph below it. A brief, localised Ca^{2+} spark is seen spreading laterally from the centre of the cell. B. Transverse line-scan image from another vessel (see cell outline and scanline position in left-hand panel) in which sparks summated to give a longer lasting global Ca^{2+} oscillation. The gap in the linescan image and fluorescence v. time plot results from the time taken for the image to be downloaded by the computer between acquisition cycles.

Europe PMC Funders Author Manuscripts

Invest Ophthalmol Vis Sci. Author manuscript; available in PMC 2008 December 01.

Table 1

	Ca^{2+} sparks		Ca^{2+} Sparks on Oscillations			Oscillations	
		n		***n***	***p***		***n***
Amplitude ($\Delta F/F_0$)	0.81 ± 0.04	102	0.69 ± 0.04	78	*	0.93 ± 0.04	162
Spread (FWHM)	1.25 ± 0.05 μm	96	1.67 ± 0.08 μm	65	***	n/a	n/a
Duration (FDHM)	23.6 ± 1.15 ms	102	22.2 ± 1.12 ms	78	*ns*	1992 ± 0.06 ms	162
Frequency	0.56 ± 0.06 s^{-1}	60 cells	2.86 ± 0.25 s^{-1}	50 cells	***	0.13 ± 0.01 s^{-1}	35 cells

Basic properties of Ca^{2+} sparks and global Ca^{2+} oscillations in retinal MVSM cells. It was generally not possible to measure the FWHM for oscillations since the majority of these events spread across the full cell width. With the exception of frequency data, 'n' represents the number of Ca^{2+} events analyzed from a minimum of 6 vessels. The statistical significance for comparisons between sparks from baseline and sparks superimposed on oscillations as follows:

ns ($p>0.05$)

* ($p<0.05$)

*** ($p<0.001$).